

# Maduramicin Rapidly Eliminates Malaria Parasites and Potentiates the Gametocytocidal Activity of the Pyrazoleamide PA21A050

Maxim I. Maron,<sup>a\*</sup> Crystal T. Magle,<sup>a\*</sup> Beata Czesny,<sup>a</sup> Benjamin A. Turturice,<sup>a\*</sup> Ruili Huang,<sup>b</sup> Wei Zheng,<sup>b</sup> Akhil B. Vaidya,<sup>c</sup> Kim C. Williamson<sup>a\*</sup>

Department of Biology, Loyola University, Chicago, Illinois, USA<sup>a</sup>; National Center for Advancing Translational Sciences, National Institutes of Health, Bethesda, Maryland, USA<sup>b</sup>; Department of Microbiology and Immunology, Center for Molecular Parasitology, Drexel University College of Medicine, Philadelphia, Pennsylvania, USA<sup>c</sup>

**New strategies targeting *Plasmodium falciparum* gametocytes, the sexual-stage parasites that are responsible for malaria transmission, are needed to eradicate this disease. Most commonly used antimalarials are ineffective against *P. falciparum* gametocytes, allowing patients to continue to be infectious for over a week after asexual parasite clearance. A recent screen for gametocytocidal compounds demonstrated that the carboxylic polyether ionophore maduramicin is active at low nanomolar concentrations against *P. falciparum* sexual stages. In this study, we showed that maduramicin has an EC<sub>50</sub> (effective concentration that inhibits the signal by 50%) of 14.8 nM against late-stage gametocytes and significantly blocks *in vivo* transmission in a mouse model of malaria transmission. In contrast to other reported gametocytocidal agents, maduramicin acts rapidly *in vitro*, eliminating gametocytes and asexual schizonts in less than 12 h without affecting uninfected red blood cells (RBCs). Ring stage parasites are cleared by 24 h. Within an hour of drug treatment, 40% of the normally crescent-shaped gametocytes round up and become spherical. The number of round gametocytes increases to >60% by 2 h, even before a change in membrane potential as monitored by MitoProbe DiIC1 (5) is detectable. Maduramicin is not preferentially taken up by gametocyte-infected RBCs compared to uninfected RBCs, suggesting that gametocytes are more sensitive to alterations in cation concentration than RBCs. Moreover, the addition of 15.6 nM maduramicin enhanced the gametocytocidal activity of the pyrazoleamide PA21A050, which is a promising new antimalarial candidate associated with an increase in intracellular Na<sup>+</sup> concentration that is proposed to be due to inhibition of PfATP4, a putative Na<sup>+</sup> pump. These results underscore the importance of cation homeostasis in sexual as well as asexual intraerythrocytic-stage *P. falciparum* parasites and the potential of targeting this pathway for drug development.**

Reports of decreasing sensitivity to artemisinin in Southeast Asia provide a sense of urgency to the development of novel antimalarial compounds (1). Although both gametocytes and asexual parasites reside within the red blood cell (RBC), their physiologies differ, resulting in various sensitivities to common antimalarial drugs (2). After RBC invasion, asexual parasites undergo four or five rounds of DNA replication, resulting in 16 to 32 new parasites every 48 h. In contrast, gametocytes do not replicate in the human host. Instead, after RBC invasion, sexual differentiation of *Plasmodium falciparum* progresses through five stages of development over the course of 10 to 12 days, resulting in a single female or male gametocyte (3). Once taken up in a blood meal by a mosquito, gametocytes are stimulated to emerge from the RBC and develop into female and male gametes (4). After fertilization, the zygote differentiates into an ookinete that migrates out of the mosquito midgut, where it forms an oocyst that produces tens of thousands of sporozoites that can infect humans during a subsequent blood meal. To prevent malaria-related mortality and block disease transmission, both asexual and sexual stage parasites need to be eliminated.

A recent screen for gametocytocidal compounds identified 7 molecules with an EC<sub>50</sub> (effective concentration that inhibits the signal by 50%) of <50 nM, including two carboxylic polyether ionophores, maduramicin and narasin (5), that transport cations across membranes, thus altering intracellular cation concentrations (6–8). Related ionophores, salinomycin and monensin, were less potent but were also found to have activity against late-stage gametocytes, which has been confirmed in an independent study (9). Both maduramicin and narasin have high affinities for monovalent cations (7, 8), including K<sup>+</sup>, Na<sup>+</sup>, and H<sup>+</sup>, and have been

used as coccidiostats in poultry and rabbits for many years (10, 11). Maduramicin is one of the newer members of this family (12), and prior to our recent screen, its effect on *Plasmodium* had not been reported, and neither compound had been tested against gametocytes.

Polyether ionophores, such as maduramicin, are large heterocyclic compounds containing a series of electronegative crown ethers that can coordinate monovalent or divalent metal ions (Fig. 1A). Ion binding causes a structural change that exposes hydrophobic methyl groups on the exterior of the molecule (Fig. 1B) (13). This allows the ionophore to associate with lipid bilayers and transport ions down their concentration gradients, thereby altering the membrane electropotential. This effect has been well stud-

Received 8 August 2015 Returned for modification 9 September 2015

Accepted 8 December 2015

Accepted manuscript posted online 28 December 2015

Citation Maron MI, Magle CT, Czesny B, Turturice BA, Huang R, Zheng W, Vaidya AB, Williamson KC. 2016. Maduramicin rapidly eliminates malaria parasites and potentiates the gametocytocidal activity of the pyrazoleamide PA21A050. *Antimicrob Agents Chemother* 60:1492–1499. doi:10.1128/AAC.01928-15.

Address correspondence to Kim C. Williamson, kim.williamson@usuhs.edu.

\* Present address: Maxim I. Maron, Albert Einstein College of Medicine, Bronx, New York, USA; Crystal T. Magle, Health Sciences Library and University of Colorado Anschutz Medical Campus, Aurora, Colorado, USA; Benjamin A. Turturice, University of Illinois College of Medicine, Chicago, Illinois, USA; Kim C. Williamson, Microbiology and Immunology Department, Uniformed Services University of the Health Sciences, Bethesda, Maryland, USA.

Copyright © 2016, American Society for Microbiology. All Rights Reserved.

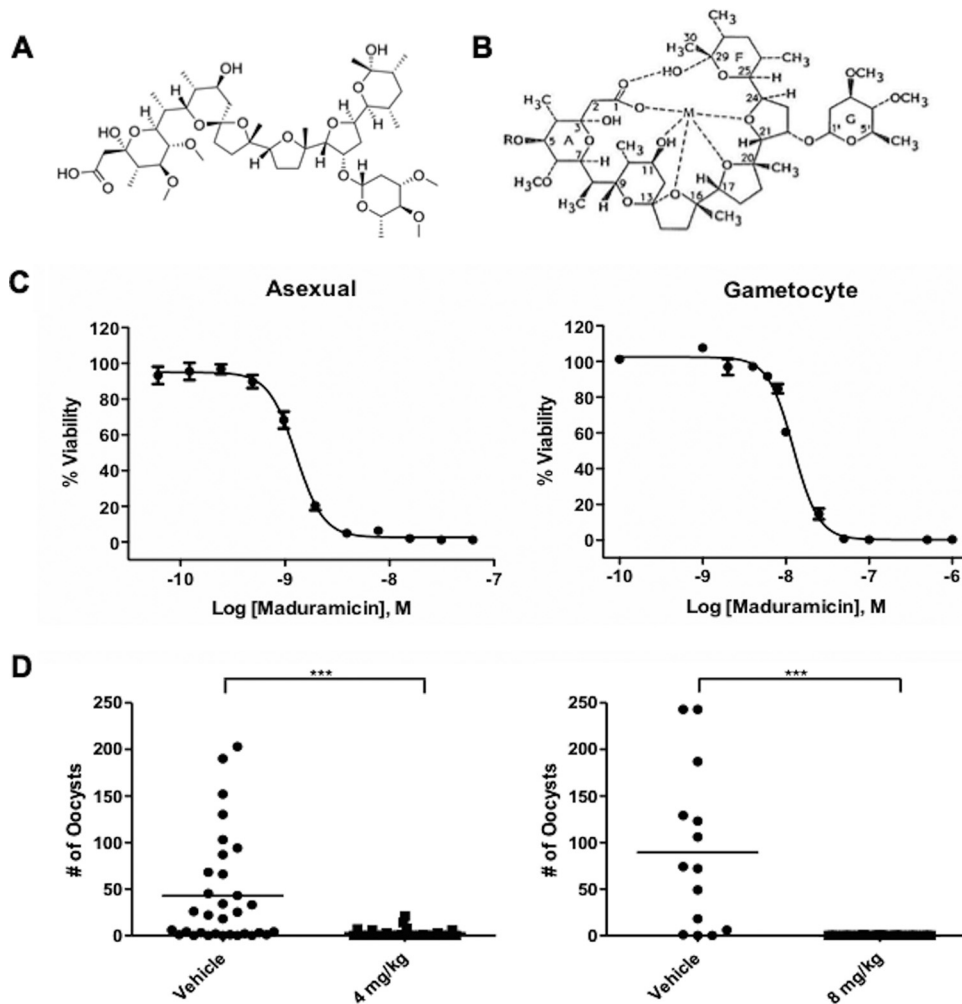


**FIG 1** (A and B) Chemical structure of maduramicin (A) and predicted structural change in the presence of a monovalent cation (M) (B). Adapted from reference 8 by permission from the publisher and the author. (C) Maduramicin dose-response curves against *P. falciparum* NF54 asexual parasites (left) and late-stage gametocytes (>80% stage IV or V) (right). The experiment was repeated three times in duplicate, and a representative graph is shown. Error bars represent the ranges of duplicate samples. (D) Transmission blocking efficacy of maduramicin in the *P. berghei*-mouse model. *A. stephensi* mosquitoes were allowed to take a blood meal from *P. berghei*-infected mice 1.5 h after i.v. treatment with 4 mg/kg or 8 mg/kg of maduramicin or a vehicle control. Ten days later, the mosquito midguts were isolated and the *P. falciparum* oocysts were counted. \*\*\*, significant difference ( $P < 0.001$ ) between two groups as determined by the Mann-Whitney U test.

ied for monensin, the first ionophore approved for veterinary use (10). Monensin carries  $\text{Na}^+$  into and  $\text{H}^+$  out of the cell, increasing intracellular  $\text{Na}^+$  concentration and decreasing intracellular  $\text{H}^+$  (13). This change then stimulates active transport by membrane-associated ATPases, such as the  $\text{Na}^+/\text{K}^+$  ATPase in mammalian cells, to attempt to restore the ionic equilibrium (14). Depending on the cell type and ionophore concentration, this attempt at re-equilibration may not be effective and can lead to cell death.

An increase in intracellular  $\text{Na}^+$  has also recently been associated with three new classes of antimalarials, spiroindolones (15, 16), pyrazoleamides (17), and dihydroisoquinolones (18), as well as 28 of the novel antimalarial compounds included in the Malaria Box (19), a small-molecule library compiled and distributed by Medicines for Malaria Venture. Mutations in PfATP4 (PF3D7\_1211900), which has homology to a P-type cation pump that could play a role in actively transporting  $\text{Na}^+$  out of the cell, have been found to confer resistance to the three new antimalarial

candidates. These findings suggest that these distinct compounds increase intracellular  $\text{Na}^+$  levels by inhibiting PfATP4 activity. The initial identification of these compounds resulted from screens performed against asexual *P. falciparum* parasites. The compounds have since been tested against late-stage gametocytes and found to have a wide range of  $\text{EC}_{50}$ s (39 to >1,000 nM) (5, 17, 20–23).

Here, we demonstrate that maduramicin completely blocks malaria transmission in an *in vivo* rodent malaria model and potentiates the gametocytocidal effects of the pyrazoleamide PA21A050 (17). *In vitro*, maduramicin rapidly alters the morphology of intraerythrocytic *P. falciparum* gametocytes and effectively eliminates them in 12 h. Intraerythrocytic asexual schizont stages are also cleared in 12 h, while asexual ring stage clearance takes longer. Maduramicin is not preferentially taken up by gametocyte-infected erythrocytes compared to uninfected erythrocytes, suggesting that parasite-specific pathways underlie the efficacy of

this compound. Together, these data demonstrate the critical importance of ion homeostasis in both asexual and sexual intraerythrocytic stages.

## MATERIALS AND METHODS

**Cell culture.** *P. falciparum* NF54 asexual parasites were cultured as described previously (24). Briefly, NF54 strain parasites were maintained in complete RPMI medium containing RPMI 1640, 25 mM HEPES, 100  $\mu\text{g ml}^{-1}$  of hypoxanthine, and 0.3 mg  $\text{ml}^{-1}$  of glutamine (KD Biomedical, Columbia, MD) supplemented with 25 mM  $\text{NaHCO}_3$  (pH 7.3), 5  $\mu\text{g ml}^{-1}$  of gentamicin, and 10% human serum (Interstate Blood Bank, Memphis, TN). Gametocyte cultures were set up at 0.2% parasitemia and 6% hematocrit. After 3 days, the hematocrit was reduced to 3% by increasing the media added during the daily feed. *N*-Acetyl-D-glucosamine (NAG; 50 mM) was added to the cultures on days 10 to 12 to eliminate asexual parasites. On day 13, gametocytes (stages III to V) were purified by flotation on a 65% Percoll-phosphate-buffered saline (PBS) or 18% NycoDenz-SA buffer cushion and returned to culture. The next day, the parasites were resuspended at 10% gametocytemia and 2% hematocrit for use in the drug assays. Stages IV and V were the predominant stages in the preparation, at >80%, with stage III gametocytes making up the remaining <20%.

**In vivo malaria transmission blocking.** *Plasmodium berghei* ANKA 2.34 parasites were maintained by serial passage in CD1 mice (Charles River). Female mice were infected by intraperitoneal injection with 200  $\mu\text{l}$  of whole blood from a *P. berghei*-infected mouse with 10% parasitemia. Two days later, a blood sample was checked for exflagellation by microscopy 10 to 20 min after the blood draw. If exflagellation was not observed, the sample was reassessed the next day. After exflagellation was observed, the mice were treated intravenously (i.v.) with drug vehicle alone (10% dimethyl sulfoxide [DMSO]–18% Cremophor RH 40–3.6% dextrose) or 4 to 8 mg/kg (of body weight) maduramicin. At 1.5 h after treatment, mice were anesthetized and 20 to 30 female *Anopheles stephensi* mosquitoes (6 to 9 days old) were allowed to feed on an infected mouse for 15 min. Mosquitoes were maintained on 5% (wt/vol) glucose at 19°C and 80% relative humidity. At day 10 postfeeding, mosquito midguts were dissected and parasite infection was measured by staining with 0.2% mercurochrome and determining the number of oocysts per midgut. Statistical significance was determined using the Mann-Whitney U test when comparing two treatment groups. All animal experiments were done at Loyola University, Chicago, IL, in compliance with the guidelines of their Institutional Animal Care and Use Committee.

**Maduramicin time course.** NF54 asexual parasites underwent two rounds of synchronization using 5% sorbitol 15 h apart (25). When the parasitemia reached 5 to 10%, the culture was distributed in duplicate to a 24-well plate at a final 2 to 3% hematocrit. A 100 nM or 10 nM concentration of analytical-grade maduramicin (Sigma-Aldrich) or 0.01% ethanol diluted in complete medium was added to each well. The cells were incubated at 37°C in 5%  $\text{CO}_2$  for the first 2 h, transferred to an atmosphere of 90%  $\text{N}_2$ , 5%  $\text{O}_2$ , and 5%  $\text{CO}_2$ , and incubated at 37°C for the remainder of the experiment. At specified times (0, 0.33, 1, 1.5, 2, 4, 8, 12, 18, and 24 h), an aliquot was taken for Giemsa-stained smears and flow cytometric analysis.

**Flow cytometric analysis.** Viability was assayed by flow cytometry using a membrane potential dye, MitoProbe DiIC1 (5) [DiIC1 (5); Thermo Scientific], which was previously described and validated by comparison with the oxidoreduction indicator alamarBlue (26). Cells were resuspended at 0.1% hematocrit in 50 nM DiIC1 (5) with SA buffer in a 96-well vee-bottom plate and incubated at 37°C in the dark for 20 to 30 min prior to analysis on an Accuri C6 flow cytometer (BD Biosciences). Uninfected RBCs incubated with DiIC1 (5) and unstained *P. falciparum* parasites were used as controls to determine the threshold for DiIC1 (5) (640-nm laser excitation and FL4 emission filter [675/25 nm])–positive, single, and intact cell populations by following the gating strategy of Malleret et al. (27). Viability was calculated by determining the ratio of

DiIC1 (5)-positive events in maduramicin-treated samples compared to vehicle controls.

**Dose-response and interaction studies.** Analytical standard-grade maduramicin (Sigma-Aldrich) was dissolved in 100% ethanol at a concentration of 50 mM and stored at 4°C. The pyrazoleamide PA21A050 (17) dissolved in DMSO at a concentration of 10 mM was kept at –20°C. A 96-well flat-bottom plate was prepared with 100  $\mu\text{l}$  of the designated compound at a 2 $\times$  concentration dissolved in complete medium. For the maduramicin-PA21A050 interaction studies, a checkerboard design was used ranging from 500 to 1.95 nM in a 2-fold dilution series. Control wells included the same concentration series of each drug alone, 0.5% ethanol, 0.5% DMSO, a combination of both carriers at 0.5% each, and 32 nM epoxomicin, a potent gametocytocidal agent. NF54 *P. falciparum* gametocytes purified as described above were set at 10% parasitemia and 2% hematocrit, while NF54 *P. falciparum* asexual parasites were set between 0.5 to 1% parasitemia and 2% hematocrit. One hundred-microliter quantities of the parasite preparations were added to the plate, resulting in a 1:2 dilution of both the hematocrit and the compound for a final concentration of 0.5% carrier (either ethanol or DMSO). Assay plates were incubated at 37°C in the dark with 5%  $\text{CO}_2$ , 5%  $\text{O}_2$ , and 90%  $\text{N}_2$  for 72 h, and viability was evaluated using the flow cytometric assay described above. Inhibition was calculated by subtracting DiIC1 (5)-positive events in maduramicin-treated samples from those in vehicle controls and dividing the resulting value by the total number of viable cells in vehicle controls.

**Maduramicin ELISA.** A commercial maduramicin enzyme-linked immunosorbent assay (ELISA) kit (Abraxis BioScience) was used to quantify maduramicin partitioning in infected and uninfected RBCs according to the manufacturer's instructions. Percoll-purified stage III to V NF54 gametocytes or uninfected RBCs suspended in complete medium were distributed in a 24-well plate at 1% hematocrit and 80% parasitemia in duplicate. Cells were incubated in 100 nM maduramicin, 10 nM maduramicin, or 0.01% ethanol in PBS (137 mM NaCl, 2.7 mM KCl, 10 mM  $\text{Na}_2\text{HPO}_4$ , and 1.8 mM  $\text{KH}_2\text{PO}_4$ ; pH 7.4) at 37°C for 2 h in an atmosphere of 5%  $\text{CO}_2$ , 5%  $\text{O}_2$ , and 90%  $\text{N}_2$ . After the 2-h incubation, cells were isolated by centrifugation (3 min at 1,860  $\times g$ ) and washed once with 1 ml of PBS (4°C, pH 7.4). The washed cell pellets were treated with 100% acetone, vortexed, and incubated on a rocker, with frequent inversion. The cells were again pelleted by centrifugation for 5 min at 3,000  $\times g$ , and 40  $\mu\text{l}$  of the supernatant was diluted 1:24 in sample diluent provided by Abraxis and transferred into a 96-well plate coated with anti-rabbit secondary antibody. Next, horseradish peroxidase (HRP)-conjugated maduramicin was added to each well, followed by rabbit anti-maduramicin primary antibody. The plate was sealed, mixed for 60 s, and then incubated at room temperature for 1 h, allowing maduramicin in the sample to compete with HRP-conjugated maduramicin for binding to the primary antibody, which is captured by the secondary antibody bound to the plate. After incubation, the plate was washed 4 times and 3,3',5,5'-tetramethylbenzidine (TMB) was added. Following a 20-min incubation in the dark at room temperature, stop solution was added and the absorbance was measured at 450 nm using a BMG Labtech FLUOstar Omega plate reader. The final signal is inversely correlated with the maduramicin concentration in the sample, indicating successful competition with the HRP-conjugated maduramicin for antibody binding. The standard curve was performed using five standards that contained 0, 0.27, 0.54, 1.1, and 2.7 ppb.

**Data analysis.** Percent viability or inhibition was calculated for each drug concentration or combination as described above. Prism software was used for statistical analysis and to calculate the effective concentrations that inhibited the signal by 50% ( $\text{EC}_{50}$ s) using the Hill equation. Maduramicin and PA21A050 interaction was determined using software developed in-house at the National Center for Advancing Translational Sciences (NCATS) based on the theoretical work of Chou (28). The concentration response series with a fixed ratio of PA21A050 over maduramicin (P/Mad; 0.062, 0.125, 0.25, 0.5, 1, 2, 4, 8, or 16) was extracted from the data matrix and fit to the Hill equation. Each  $\text{EC}_{50}$  was decomposed into component  $\text{EC}_{50}$ s for PA21A050 and maduramicin based on the P/Mad

ratio. The component  $EC_{50}$ s were further normalized to the single-agent  $EC_{50}$ s of PA21A050 and maduramicin, respectively, generating the fractional inhibitory concentration (FIC). The FICs from the four runs were averaged. The isobologram in Fig. 4 is a plot of the FIC of one combination drug (PA21A050) against the other (maduramicin).

## RESULTS AND DISCUSSION

**Maduramicin is a potent inhibitor of asexual and gametocyte *P. falciparum* parasites.** A recent screen for gametocytocidal agents demonstrated for the first time the efficacy of polyether ionophores against the transmission stages of *P. falciparum* (5). The most potent was maduramicin, which had a gametocytocidal  $EC_{50}$  of <50 nM against 3 parasite strains (3D7, HB3, and Dd2) with different drug sensitivities and geographic origins. Importantly, maduramicin was also >750 times less active against mammalian HepG2 cells (5). The anti-asexual parasite activity of this ionophore had not been reported previously; therefore, we first compared the *in vitro*  $EC_{50}$  against asexual parasites and stage III to V gametocytes using flow cytometry to assess viability 72 h after maduramicin treatment. Maduramicin was effective against both stages (asexual  $EC_{50}$ ,  $1.3 \pm 0.1$  nM, and stage III to V gametocyte  $EC_{50}$ ,  $14.8 \pm 1.4$  nM [Fig. 1C]), suggesting that it could block parasite transmission as well as clinical symptoms.

Several other mammalian tumor cells, including human rhabdomyosarcomas (RD) and mouse myoblasts (C2C12), have been reported to remain >80% viable after 72 h of treatment with 1  $\mu$ M maduramicin (29). The reason for the differential maduramicin sensitivities of apicomplexans, like *P. falciparum* and coccidia, and mammalian cells remains unknown, but it has allowed the use of maduramicin as a coccidiostat in animals. The standard dose used by the poultry industry for chicken feed is 5 to 7 mg/kg, which has been found to result in levels of maduramicin of ~100 nM in muscle, with no toxic effects on chickens or other nontarget species (29–31). Maduramicin treatment has a serum half-life of 13 h in chickens and does not interfere with vaccination responses, indicating that it did not affect the function of antigen-presenting cells or leukocyte activation and proliferation, which are required for the induction of immunity (31). However, accidental consumption of a large amount of maduramicin by humans (>1g/kg) and other species can result in acute toxicity (11, 32). Further preclinical testing is required to determine the health effects of short-term exposure to the nanomolar levels of maduramicin needed to clear gametocytes. To begin to test *in vivo* efficacy, we used the rodent malaria agent, *P. berghei*, in mice.

***In vivo* transmission blocking activity.** The ability of maduramicin to block malaria transmission *in vivo* using the *P. berghei*-mouse model was evaluated. In contrast to the 10 to 12 days required for *P. falciparum* gametocytes to develop through five morphologically distinct stages, *P. berghei* gametocytes mature in 24 h and remain round throughout differentiation. Therefore, to assess maturation, the ability of male gametocytes to exflagellate was monitored. Once exflagellation was detected, maduramicin was administered and *A. stephensi* mosquitoes were allowed to take blood meals from the infected mice 1.5 h posttreatment. Oocyst production 10 days later was significantly ( $P < 0.001$ ) decreased at both maduramicin dosages compared to that for mosquitoes that fed on mice treated with carrier alone (Fig. 1D).

**Maduramicin rapidly triggers distinct morphological changes in mature gametocytes and asexual *P. falciparum* parasites.** The short *in vivo* treatment time (1.5 h) needed to success-

fully block transmission suggests that maduramicin has a rapid effect on parasite viability. To evaluate this directly in *P. falciparum*, the effect of 100 nM maduramicin on the *in vitro* viability of stage IV and V gametocytes as well as ring and schizont stage asexual parasites was monitored from 0.33 to 24 h.

Within an hour of applying drug to *in vitro* *P. falciparum* cultures, changes in viability as measured by the membrane potential dye DiIC1 (5) and morphology were apparent in both sexual stage and asexually developing parasites. Viability fell below 80% by 4 h and declined to <10% by 12 h for schizonts and late-stage gametocytes; in ring stages, this occurred at the 24-h time point (Fig. 2A). These findings are in marked contrast to those obtained with other gametocytocidal agents, such as the diaminonaphthoquinones (DANQs) and the proteasome inhibitor epoxomicin, which require 72 h to decrease late-stage gametocyte viability to <10% (26). The similar time courses of the decrease in membrane potential following maduramicin treatment of late-stage gametocytes and asexual *Plasmodium* parasites suggests that asexual parasite-specific cellular activities, such as hemoglobin digestion, DNA replication, or the presence of a plasmodial surface anion channel (PSAC) on the RBC surface, do not influence the efficacy of maduramicin (33–36). These processes have previously been identified as targets for compounds that preferentially affect asexual parasites, including pyrimethamine, chloroquine, and furosemide.

Although the efficacies and time courses were similar for the different parasite stages, distinct changes in morphology were observed, which is consistent with their unique physiologies (Fig. 2B). Just 1 h after treatment with 100 nM maduramicin, 40% of gametocytes had rounded up, compared to just 10 to 15% in control samples (Fig. 2C). The fraction of round gametocytes remained at 10 to 15% in control wells, while this percentage increased to >60% at 4 h and reached almost 100% at 8 h in samples treated with maduramicin (Fig. 2C). In contrast, ring stages appeared to have undergone developmental arrest at the 4-h time point, followed by a progressive decrease in size, resulting in dense blue bodies apparent at 12 h (Fig. 2B). Schizont stages also appeared to stop developing 1 h after treatment with maduramicin. Then, the cytoplasmic contents consolidated into dense aggregates and the parasite shrank until, as with the case with ring stages, only dense blue bodies remained at 12 h (Fig. 2B). No changes were observed in the uninfected RBCs through the 48-h course of the experiment. Once specific markers for different forms of cell death are established for *P. falciparum*, reevaluating maduramicin-induced death with these markers would be interesting (37).

Rounding up is usually considered a physiological response of mature, stage V *P. falciparum* gametocytes that is stimulated within minutes of the transition from the vertebrate to insect host and is mediated by cGMP (38). The lack of other signs of gametogenesis, such as male exflagellation, coupled with the progressive increase in vacuolation, decrease in staining intensity, morphological evidence of ruptured gametes, scattered pigment, and ultimately clearance of the gametocytes in 12 h, is consistent with the altered morphology being due to an osmotic change, not an active process. Maduramicin-induced rounding is distinct from the response of late-stage gametocytes to the proteasome inhibitor epoxomicin. Following epoxomicin treatment, gametocytes retain their elongated shape but shrink in diameter, ultimately resembling a needle before disintegrating (39). Hliscs et al. have

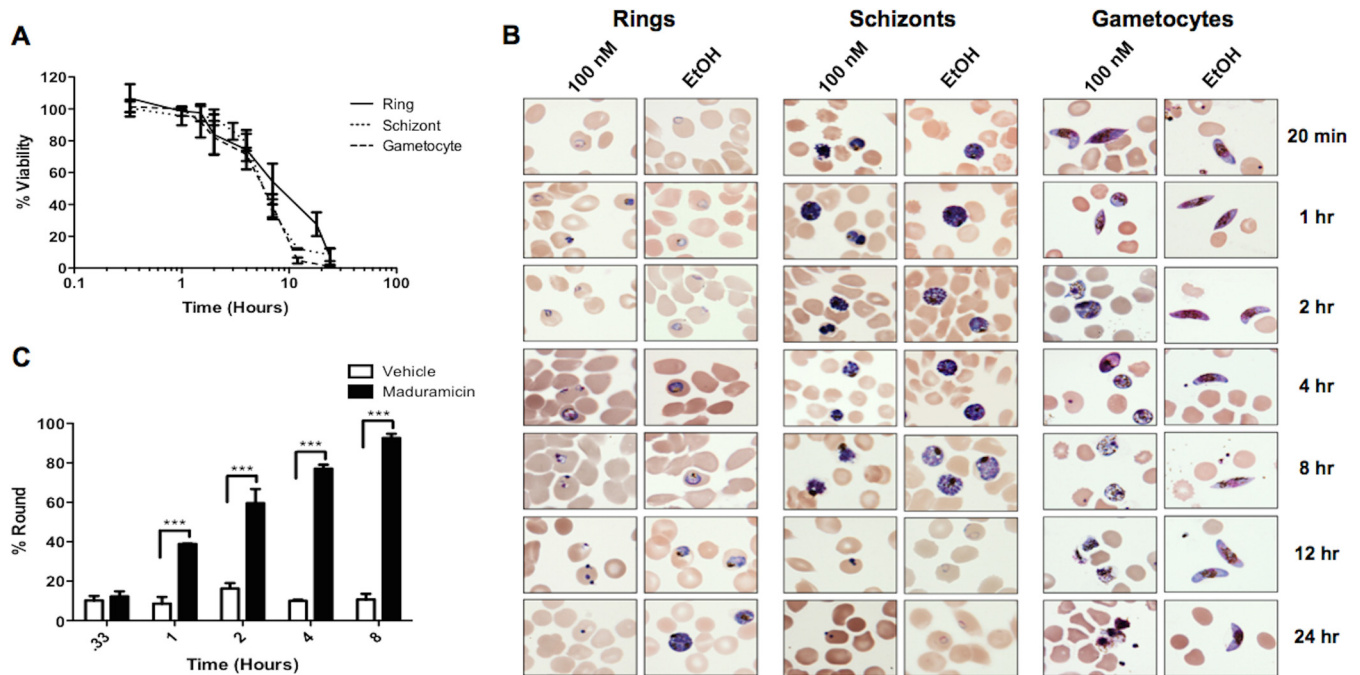


**FIG 2** (A) Time course of *P. falciparum* NF54 parasite viability after maduramicin treatment. The viability of synchronized preparations of ring, schizont, or stage IV or V gametocytes following the addition of 100 nM maduramicin was monitored periodically for 24 h using flow cytometry and MitoProbe DiIC1 (5). Viability was calculated by determining the ratio of DiIC1 (5)-positive events in maduramicin-treated samples compared to vehicle controls. The data are the means of two independent trials with two duplicates. The error bars show the standard deviations. (B) Morphological analysis of *P. falciparum* parasites through the time course shown in panel A. Shown are representative images of Giemsa-stained smears made at the times indicated on the right from cultures set up with rings, schizonts, or stage IV or V gametocytes following the addition of 100 nM maduramicin or a vehicle control, 0.01% ethanol (EtOH). (C) Quantification of round gametocytes. The percentage of round gametocytes was determined by counting gametocytes on smears prepared from cultures at the indicated times after treatment with 100 nM maduramicin or a vehicle control, 0.01% EtOH. The average percentages, with error bars representing the ranges from two independent trials, are plotted. Significance was determined using two-way analysis of variance (ANOVA) and Bonferroni posttests. \*\*\*,  $P < 0.001$ .

recently shown that tubulin and actin remain in complexes in stage V gametocytes (40), but the changes in the cytoskeleton during rounding were not evaluated. Further work is needed to define the mechanisms involved in this transition from an elongated, sausage-like shape to an energetically favorable sphere. The decrease in DiIC1 (5) signal lags slightly behind the shape change, falling below 80% at 4 h, which indicates that rounding is a more sensitive marker of the changes induced by ionophore treatment than the loss in membrane or mitochondrial potential. Rounding could be a direct response to the ionophore-induced disruption of the ion gradient across cellular membranes, while more time is needed to alter the membrane and mitochondrial membrane potential enough to be detected by a change in DiIC1 (5) accumulation (33). The DiIC1 (5) signal continues to decline over the next 12 h, corresponding to the disappearance of parasites from Giemsa-stained smears of the maduramicin cultures, while the uninfected RBCs remain intact. A similar time course for mitochondrial toxicity was found in another apicomplexan parasite, *Toxoplasma gondii*, using the related ionophore monensin, which, like maduramicin, has a high affinity for monovalent cations and is able to transport  $\text{Na}^+$  down its concentration gradient into cells (8, 14, 41).

**Maduramicin does not preferentially partition into infected RBCs.** Previous studies have demonstrated a significant difference between the lipid composition of uninfected and infected erythrocytes, raising the possibility of differences in maduramicin

binding (42). For instance, uninfected RBCs do not contain cardiolipin, a diphosphatidylglycerol lipid present only in the inner membrane of the mitochondria, while sphingomyelin levels are twice as high in uninfected RBCs as in infected RBCs. A competitive maduramicin-specific ELISA was used to quantify drug levels in *P. falciparum* gametocytes and uninfected RBCs after 2 h of incubation with or without 100 nM maduramicin. A 2-h exposure was chosen because the gametocytes were still viable at that time. Maduramicin levels significantly increased in both gametocytes and uninfected RBCs after treatment compared to the amount in untreated controls ( $P < 0.001$ ), but no difference was observed between uninfected and infected RBCs ( $P > 0.05$ ) (Fig. 3). These data strongly indicate that drug levels do not contribute to the specificity of maduramicin for *P. falciparum* over RBCs; rather, it is more likely that the intraerythrocytic stage parasites are more sensitive to the alterations in ion flux induced by maduramicin.

**Maduramicin potentiates PA21A050 gametocytocidal activity.** The sensitivity of *P. falciparum* parasites to increases in intracellular  $\text{Na}^+$  levels has recently been demonstrated to be a common property of several classes of antimalarial drugs believed to act through inhibition of a P-type  $\text{Na}^+$  ATPase, PfATP4 (16–18, 23). The potential for PfATP4 inhibitors to block the parasite's adaptive response to the ion flux induced by maduramicin and augment the effects of increases in intracellular  $\text{Na}^+$  concentration prompted us to test for synergy between these compounds.

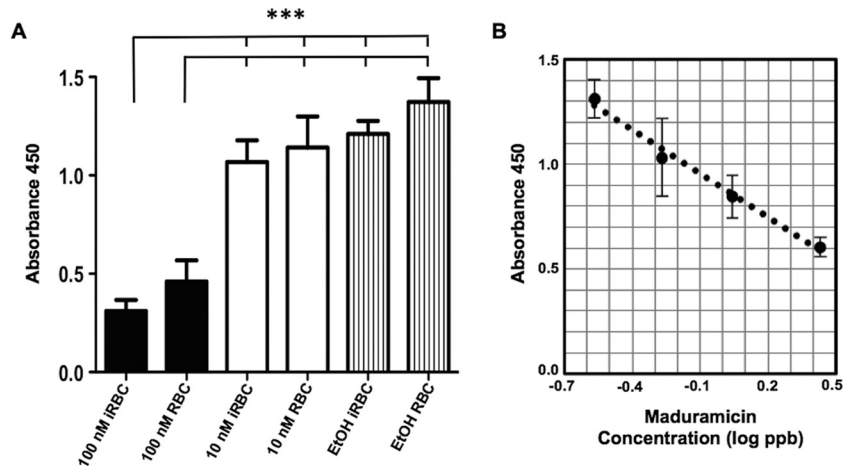


**FIG 3** ELISA quantification of maduramicin. (A) Stage IV or V gametocyte-infected (iRBC) and uninfected (RBC) RBCs were harvested 2 h after the addition of a vehicle control (0.01% EtOH) or 10 nM or 100 nM maduramicin, washed, and extracted in acetone. Maduramicin levels in the acetone extract were quantified by a commercial competitive ELISA kit (Abraxis); the average absorbance values from two independent trials with duplicates are plotted. The error bars represent the standard deviations. Significance was determined using one-way ANOVA followed by Bonferroni's multiple-comparison test. \*\*\*,  $P < 0.001$ . (B) ELISA quantification of maduramicin standards. Average absorbance values for maduramicin standards from two independent trials with duplicates are plotted against the log of the maduramicin concentration in parts per billion. The error bars represent the standard deviations.  $R^2 = 0.989$ .

To evaluate this hypothesis, we simultaneously administered the pyrazoleamide PA21A050 and maduramicin at a range of doses and calculated the FIC (43). The left shift of the curve on the PA21A050 FIC/maduramicin FIC plot is consistent with synergy between the compounds (Fig. 4A). Importantly, adding 15.6 nM maduramicin ( $EC_{50}$ ) to 15.6 nM PA21A050 decreased gametocyte viability to  $<11\%$  from  $>97.5\%$  viability with 15.6 nM PA21A050 alone (Fig. 4B and C), enhancing efficacy  $\sim 10$ -fold. These results demonstrate the effectiveness of combining compounds that increase the intracellular  $Na^+$  concentration through different

mechanisms and suggest an important approach to enhance the transmission blocking activity of these inhibitors.

**Conclusion.** Here we show that maduramicin works quickly, blocking transmission *in vivo* and significantly eliminating viable gametocytes and schizont stage asexual parasites in 12 h. Importantly, we show synergy between maduramicin and the pyrazoleamide PfATP4 inhibitor PA21A050, which is a current candidate for antimalarial drug development. From these data, we conclude that cation homeostasis is crucial to parasite viability, and we also highlight the effectiveness of compounds that interfere with so-

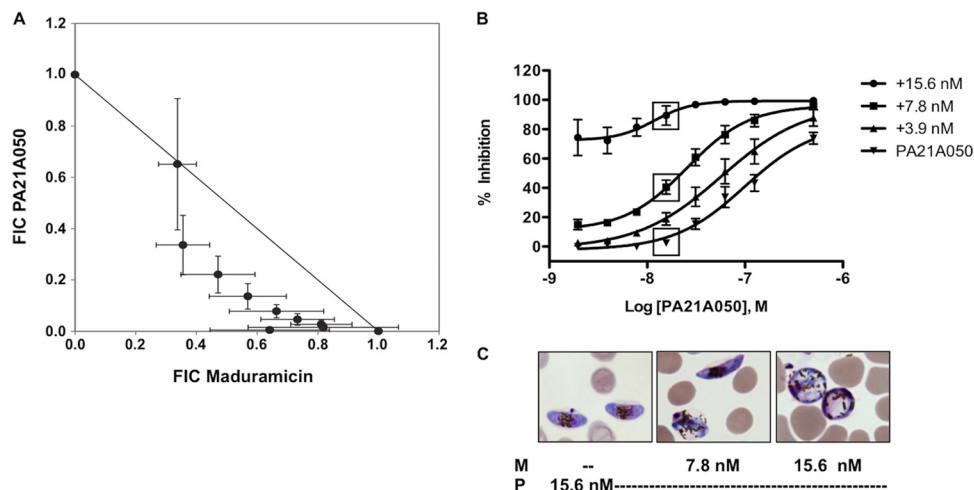


**FIG 4** (A) Isobologram of the fractional inhibitory concentration (FIC) of maduramicin and PA21A050 calculated from the fixed-ratio concentration response series. The error bars represent the standard deviations. (B) PA21A050 dose-response curves against stage III to V gametocytes in the presence and absence of maduramicin. The inhibition of stage III to V gametocyte viability was determined using flow cytometry and DiIC1 (5) after incubation with the indicated PA21A050 and maduramicin concentrations. Inhibition was calculated by subtracting DiIC1 (5)-positive events in maduramicin-treated samples from the value for vehicle controls and dividing the resulting value by total viable cells in vehicle controls. The mean inhibition of three independent trials, one of which had two duplicates, is plotted; the error bars represent the standard errors of the means. The boxes indicate the conditions used for the samples shown in panel C. (C) Representative images of Giemsa-stained smears of gametocytes after inhibition with 15.6 nM PA21A050 (P) in the absence or presence of 7.8 or 15.6 nM maduramicin (M).

dium homeostasis as potent inhibitors of *P. falciparum* development.

## FUNDING INFORMATION

The National Institute of Allergy and Infectious Diseases (NIAID) provided funding to Kim C. Williamson and Akhil B. Vaidya under grant numbers AI101396 (K.C.W.), AI114761 (K.C.W.), and AI098413 (A.B.V.). The National Center for Advancing Translational Sciences (NCATS) provided intramural funding to Wei Zheng. M.I.M. received support from a Carbon Research Scholarship.

The funders had no role in study design, data collection and interpretation, or the decision to submit the work for publication.

## REFERENCES

- Ashley EA, Dhorda M, Fairhurst RM, Amaratunga C, Lim P, Suon S, Sreng S, Anderson JM, Mao S, Sam B, Sopha C, Chuor CM, Nguon C, Sovannaroeth S, Pukrittayakamee S, Jittamala P, Chotivanich K, Chutasmit K, Suchatsoonthorn C, Runcharoen R, Hien TT, Thuy-Nhien NT, Thanh NV, Phu NH, Htut Y, Han KT, Aye KH, Mokuolu OA, Olaosebikan RR, Folaranmi OO, Mayxay M, Khanthavong M, Hongy-anthong B, Newton PN, Onyamboko MA, Fanello CI, Tshetu AK, Mishra N, Valecha N, Phyo AP, Nosten F, Yi P, Tripura R, Borrmann S, Bashraheil M, Peshu J, Faiz MA, Ghose A, Hossain MA, Samad R, Rahman MR, Hasan MM, Islam A, Miotto O, Amato R, MacInnis B, Stalker J, Kwiatkowski DP, Bozdech Z, Jeeyapant A, Cheah PY, Sakulthaew T, Chalk J, Intharabut B, Silamut K, Lee SJ, Vihokhern B, Kunasol C, Imwong M, Tarning J, Taylor WJ, Yeung S, Woodrow CJ, Flegg JA, Das D, Smith J, Venkatesan M, Plowe CV, Stepniewska K, Guerin PJ, Dondorp AM, Day NP, White NJ, Tracking Resistance to Artemisinin Collaboration (TRAC). 2014. Spread of artemisinin resistance in *Plasmodium falciparum* malaria. *N Engl J Med* 371:411–423. <http://dx.doi.org/10.1056/NEJMoa1314981>.
- Williamson KC. 2008. New antimalarials targeting both the asexual and gametocyte stages. *Drugs Future* 33:1033. <http://dx.doi.org/10.1358/dof.2008.33.12.1287737>.
- Alano P, Carter R. 1990. Sexual differentiation in malaria parasites. *Annu Rev Microbiol* 44:429–449. <http://dx.doi.org/10.1146/annurev.mi.44.100190.002241>.
- Kuehn A, Pradel G. 2010. The coming-out of malaria gametocytes. *J Biomed Biotechnol* 2010:976827.
- Sun W, Tanaka TQ, Magle CT, Huang W, Southall N, Huang R, Dehdashti SJ, McKew JC, Williamson KC, Zheng W. 2014. Chemical signatures and new drug targets for gametocytocidal drug development. *Sci Rep* 4:3743.
- Liu C-M, Hermann T, Downey A, Prosser BLT, Schildknecht E, Paleroni N, Westley J, Miller P. 1983. Novel polyether antibiotics X-14868A, B, C, and D produced by a *Nocardia*. Discovery, fermentation, biological as well as ionophore properties and taxonomy of the producing culture. *J Antibiot* 36:343–350.
- Caughey B, Painter NR, Gibbons WA. 1986. Equilibrium cation binding selectivity of the carboxylic ionophore narasin A: a comparison with transport selectivities reported in two biological test systems. *Biochem Pharmacol* 35:4103–4105. [http://dx.doi.org/10.1016/0006-2952\(86\)90035-3](http://dx.doi.org/10.1016/0006-2952(86)90035-3).
- Ellestad GA, Canfield N, Leese RA, Morton GO, James JC, Siegel MM, McGahren WJ. 1986. Chemistry of maduramicin. I. Salt formation and normal ketalization. *J Antibiot (Tokyo)* 39:447–456.
- D'Alessandro S, Corbett Y, Ilboudo D, Misiano P, Dahiya N, Abay SM, Habluetzel A, Grande R, Gismondo MR, Dechering KJ, Koolend KMJ, Sauerweine RW, Taramellia D, Basilicof N, Parapinia S. 2015. Salinomycin and other ionophores as new class of antimalarial drugs with transmission blocking activity. *Antimicrob Agents Chemother* 59:5135–5144. <http://dx.doi.org/10.1128/AAC.04332-14>.
- Chapman HD, Jeffers TK, Williams RB. 2010. Forty years of monensin for the control of coccidiosis in poultry. *Poult Sci* 89:1788–1801. <http://dx.doi.org/10.3382/ps.2010-00931>.
- Dorne JL, Fernandez-Cruz ML, Bertelsen U, Renshaw DW, Peltonen K, Anadon A, Feil A, Sanders P, Wester P, Fink-Gremmels J. 2013. Risk assessment of coccidiostats during feed cross-contamination: animal and human health aspects. *Toxicol Appl Pharmacol* 270:196–208. <http://dx.doi.org/10.1016/j.taap.2010.12.014>.
- Folz SD, Lee BL, Nowakowski LH, Conder GA. 1988. Anticoccidial evaluation of halofuginone, lasalocid, maduramicin, monensin and salinomycin. *Vet Parasitol* 28:1–9. [http://dx.doi.org/10.1016/0304-4017\(88\)90013-1](http://dx.doi.org/10.1016/0304-4017(88)90013-1).
- Pressman BC. 1976. Biological applications of ionophores. *Annu Rev Biochem* 45:501–530. <http://dx.doi.org/10.1146/annurev.bi.45.070176.002441>.
- Wang Z, Suo X, Xia X, Shen J. 2006. Influence of monensin on cation influx and Na<sup>+</sup>-K<sup>+</sup>-ATPase activity of *Eimeria tenella* sporozoites in vitro. *J Parasitol* 92:1092–1096. <http://dx.doi.org/10.1645/GE-783R.1>.
- Rottmann ME, McNamara C, Yeung BK, Lee MC, Zou B, Russell B, Seitz P, Plouffe DM, Dharia NV, Tan J, Cohen SB, Spencer KR, González-Páez GE, Lakshminarayana SB, Goh A, Suwanarusk R, Jegla T, Schmitt EK, Beck HP, Brun R, Nosten F, Renia L, Dartois V, Keller TH, Fidock DA, Winzeler EA, Diagana TT. 2010. Spiroindolones, a potent compound class for the treatment of malaria. *Science* 329:1175–1180. <http://dx.doi.org/10.1126/science.1193225>.
- Spillman NJ, Allen RJ, McNamara CW, Yeung BK, Winzeler EA, Diagana TT, Kirk K. 2013. Na<sup>+</sup> regulation in the malaria parasite *Plasmodium falciparum* involves the cation ATPase PfATP4 and is a target of the spiroindolone antimalarials. *Cell Host Microbe* 13:227–237. <http://dx.doi.org/10.1016/j.chom.2012.12.006>.
- Vaidya AB, Morrisey JM, Zhang Z, Das S, Daly TM, Otto TD, Spillman NJ, Wyvrat M, Siegl P, Marfurt J, Wirjanata G, Sebayang BF, Price RN, Chatterjee A, Nagle A, Stasiak M, Charman SA, Angulo-Barturen I, Ferrer S, Jiménez-Díaz MB, Santos Martínez M, Gamo FJ, Avery VM, Ruecker A, Delves M, Kirk K, Berriman M, Kortagere S, Burrows J, Fan E, Bergman LW. 2014. Pyrazoleamide compounds are potent antimalarials that target Na<sup>+</sup> homeostasis in intraerythrocytic *Plasmodium falciparum*. *Nat Commun* 5:5521. <http://dx.doi.org/10.1038/ncomms6521>.
- Jiménez-Díaz MB, Ebert D, Salinas Y, Pradhan A, Lehane AM, Myrand-Lapierre ME, O'Loughlin KG, Shackleford DM, Justino de Almeida M, Carrillo AK, Clark JA, Dennis AS, Diep J, Deng X, Duffy S, Endsley AN, Fedewa G, Guiguemde WA, Gómez MG, Holbrook G, Horst J, Kim CC, Liu J, Lee MC, Matheny A, Martínez MS, Miller G, Rodríguez-Alejandre A, Sanz L, Sigal M, Spillman NJ, Stein PD, Wang Z, Zhu F, Waterson D, Knapp S, Shelat A, Avery VM, Fidock DA, Gamo FJ, Charman SA, Mirsalis JC, Ma H, Ferrer S, Kirk K, Angulo-Barturen I, Kyle DE, DeRisi JL, Floyd DM, Guy RK. 2014. (+)-SJ733, a clinical candidate for malaria that acts through ATP4 to induce rapid host-mediated clearance of *Plasmodium*. *Proc Natl Acad Sci U S A* 111:E5455–5462. <http://dx.doi.org/10.1073/pnas.1414221111>.
- Lehane AM, Ridgway MC, Baker E, Kirk K. 2014. Diverse chemotypes disrupt ion homeostasis in the malaria parasite. *Mol Microbiol* 94:327–339. <http://dx.doi.org/10.1111/mmi.12765>.
- Bowman JD, Merino EF, Brooks CF, Striepen B, Carlier PR, Cassera MB. 2014. Antiapicoplast and gametocytocidal screening to identify the mechanisms of action of compounds within the Malaria Box. *Antimicrob Agents Chemother* 58:811–819. <http://dx.doi.org/10.1128/AAC.01500-13>.
- Sanders NG, Sullivan DJ, Mlambo G, Dimopoulos G, Tripathi AK. 2014. Gametocytocidal screen identifies novel chemical classes with *Plasmodium falciparum* transmission blocking activity. *PLoS One* 9:e105817. <http://dx.doi.org/10.1371/journal.pone.0105817>.
- Duffy S, Avery VM. 2013. Identification of inhibitors of *Plasmodium falciparum* gametocyte development. *Malar J* 12:408. <http://dx.doi.org/10.1186/1475-2875-12-408>.
- White NJ, Pukrittayakamee S, Phyo AP, Rueangweeraayut R, Nosten F, Jittamala P, Jeeyapant A, Jain JP, Lefevre G, Li R, Magnusson B, Diagana TT, Leong FJ. 2014. Spiroindolone KAE609 for *falciparum* and *vivax* malaria. *N Engl J Med* 371:403–410. <http://dx.doi.org/10.1056/NEJMoa1315860>.
- Trager W, Jensen JB. 1976. Human malaria parasites in continuous culture. *Science* 193:673–675. <http://dx.doi.org/10.1126/science.781840>.
- Lambros C, Vanderberg JP. 1979. Synchronization of *Plasmodium falciparum* erythrocytic stages in culture. *J Parasitol* 65:418–420. <http://dx.doi.org/10.2307/3280287>.
- Tanaka TQ, Guiguemde WA, Barnett DS, Maron MI, Min J, Connelly MC, Suryadevara PK, Guy RK, Williamson KC. 2015. Potent *Plasmodium falciparum* gametocytocidal activity of diamionaphthoquinones, lead antimalarial chemotypes identified in an antimalarial compound screen. *Antimicrob Agents Chemother* 59:1389–1397. <http://dx.doi.org/10.1128/AAC.01930-13>.
- Malleret B, Claser C, Ong AS, Suwanarusk R, Sriprawat K, Howland

- SW, Russell B, Nosten F, Renia L. 2011. A rapid and robust tri-color flow cytometry assay for monitoring malaria parasite development. *Sci Rep* 1:118.
28. Chou TC. 2006. Theoretical basis, experimental design, and computerized simulation of synergism and antagonism in drug combination studies. *Pharmacol Rev* 58:621–681. <http://dx.doi.org/10.1124/pr.58.3.10>.
  29. Chen X, Gu Y, Singh K, Shang C, Barzegar M, Jiang S, Huang S. 2014. Maduramicin inhibits proliferation and induces apoptosis in myoblast cells. *PLoS One* 9:e115652. <http://dx.doi.org/10.1371/journal.pone.0115652>.
  30. Kennedy DG, Blanchflower WJ, O'Dornan BC. 1997. Development of an ELISA for maduramicin and determination of the depletion kinetics of maduramicin residues in poultry. *Food Addit Contam* 14:27–33. <http://dx.doi.org/10.1080/02652039709374494>.
  31. US Food and Drug Administration. 2009. FOIA drug summaries—NADA 139-075 CYGRO; 1% type A medicated article—original approval. US Food and Drug Administration, Washington, DC. <http://www.fda.gov/AnimalVeterinary/Products/ApprovedAnimalDrugProducts/FOIADrugSummaries/ucml111243.htm>.
  32. Sharma N, Bhalla A, Varma S, Jain S, Singh S. 2005. Toxicity of maduramicin. *Emerg Med J* 22:880–882. <http://dx.doi.org/10.1136/emj.2004.020883>.
  33. Butcher GA. 1997. Antimalarial drugs and the mosquito transmission of *Plasmodium*. *Int J Parasitol* 27:975–987. [http://dx.doi.org/10.1016/S0020-7519\(97\)00079-9](http://dx.doi.org/10.1016/S0020-7519(97)00079-9).
  34. Lisk G, Kang M, Cohn JV, Desai SA. 2006. Specific inhibition of the plasmodial surface anion channel by dantrolene. *Eukaryot Cell* 5:1882–1893. <http://dx.doi.org/10.1128/EC.00212-06>.
  35. Go ML, Liu M, Wilairat P, Rosenthal PJ, Saliba KJ, Kirk K. 2004. Antiplasmodial chalcones inhibit sorbitol-induced hemolysis of *Plasmodium falciparum*-infected erythrocytes. *Antimicrob Agents Chemother* 48:3241–3245. <http://dx.doi.org/10.1128/AAC.48.9.3241-3245.2004>.
  36. Saul A, Graves P, Edser L. 1990. Refractoriness of erythrocytes infected with *Plasmodium falciparum* gametocytes to lysis by sorbitol. *Int J Parasitol* 20:1095–1097. [http://dx.doi.org/10.1016/0020-7519\(90\)90056-S](http://dx.doi.org/10.1016/0020-7519(90)90056-S).
  37. Engelbrecht D, Durand PM, Coetzer TL. 2012. On programmed cell death in *Plasmodium falciparum*: status quo. *J Trop Med* 2012:646534.
  38. McRobert L, Taylor CJ, Deng W, Fivelman QL, Cummings RM, Polley SD, Billker O, Baker DA. 2008. Gametogenesis in malaria parasites is mediated by the cGMP-dependent protein kinase. *PLoS Biol* 6:e139. <http://dx.doi.org/10.1371/journal.pbio.0060139>.
  39. Czesny B, Goshu S, Cook JL, Williamson KC. 2009. The proteasome inhibitor epoxomicin has potent *Plasmodium falciparum* gametocytocidal activity. *Antimicrob Agents Chemother* 53:4080–4085. <http://dx.doi.org/10.1128/AAC.00088-09>.
  40. Hliscs M, Millet C, Dixon MW, Siden-Kiamos I, McMillan P, Tilley L. 2015. Organization and function of an actin cytoskeleton in *Plasmodium falciparum* gametocytes. *Cell Microbiol* 17:207–225. <http://dx.doi.org/10.1111/cmi.12359>.
  41. Lavine MD, Arrizabalaga G. 2012. Analysis of monensin sensitivity in *Toxoplasma gondii* reveals autophagy as a mechanism for drug induced death. *PLoS One* 7:e42107. <http://dx.doi.org/10.1371/journal.pone.0042107>.
  42. Hsiao LL, Howard RJ, Aikawa M, Taraschi TF. 1991. Modification of host cell membrane lipid composition by the intra-erythrocytic human malaria parasite *Plasmodium falciparum*. *Biochem J* 274(Part 1):121–132.
  43. Chou TC. 2010. Drug combination studies and their synergy quantification using the Chou-Talalay method. *Cancer Res* 70:440–446. <http://dx.doi.org/10.1158/0008-5472.CAN-09-1947>.